

# **FAST IGNITION AT VERY HIGH ENERGY**

**C. Deutsch<sup>1</sup> and J.-P. Didelez<sup>2</sup>**

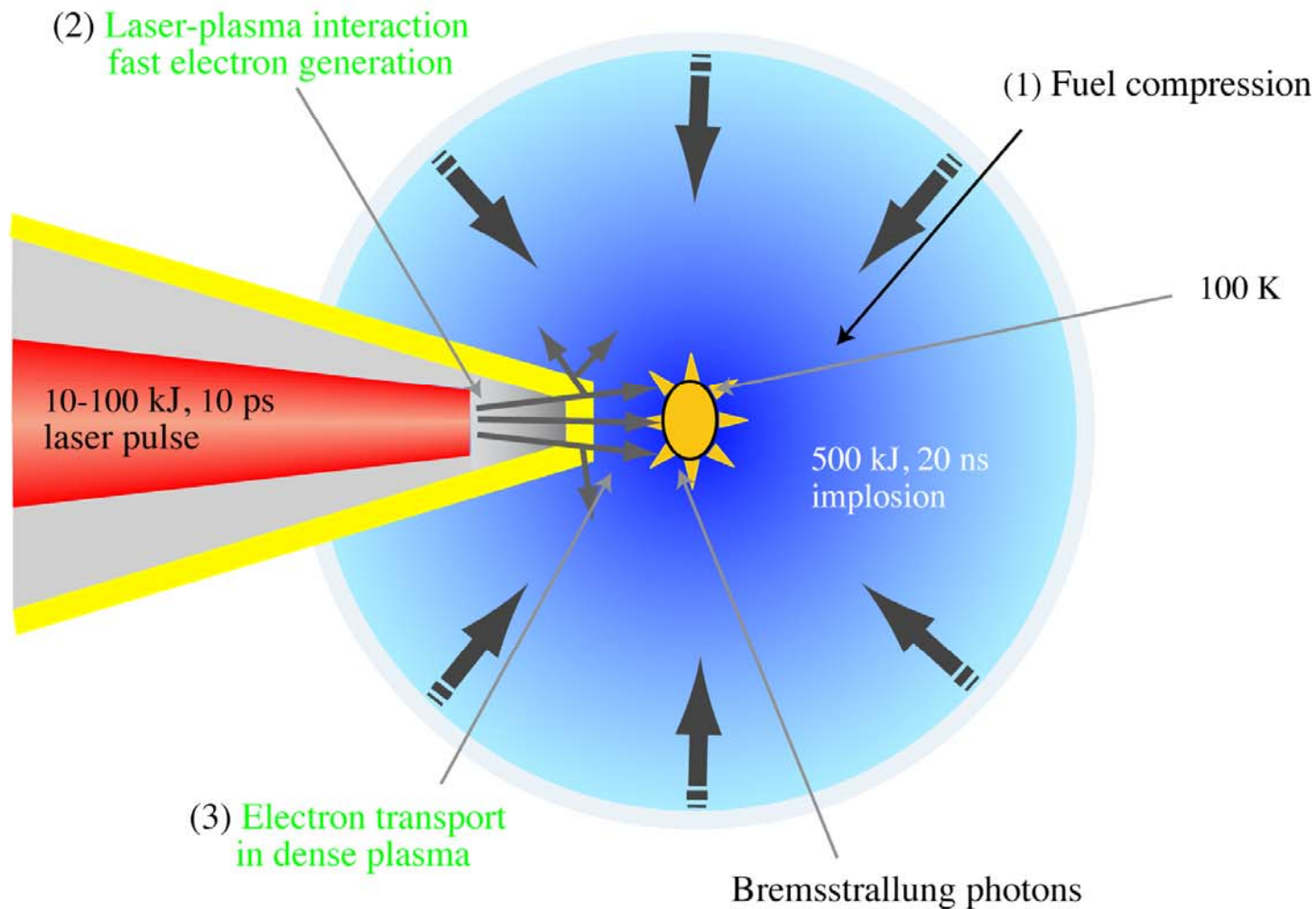
**<sup>1</sup>LPGP UParis XI - 91405 Orsay, France**

**<sup>2</sup>IPN - UParis XI - 91405 Orsay, FRANCE**

**5th INTERNATIONAL CONFERENCE ON THE FRONTIERS  
OF PLASMA PHYSICS and TECHNOLOGY**

**SINGAPORE, 18-22 April 2011**

# Cone-guided fast ignition with $\gamma$ -production, through REB-Au interaction



# High Z and $\gamma$ triggered Inelastic Production

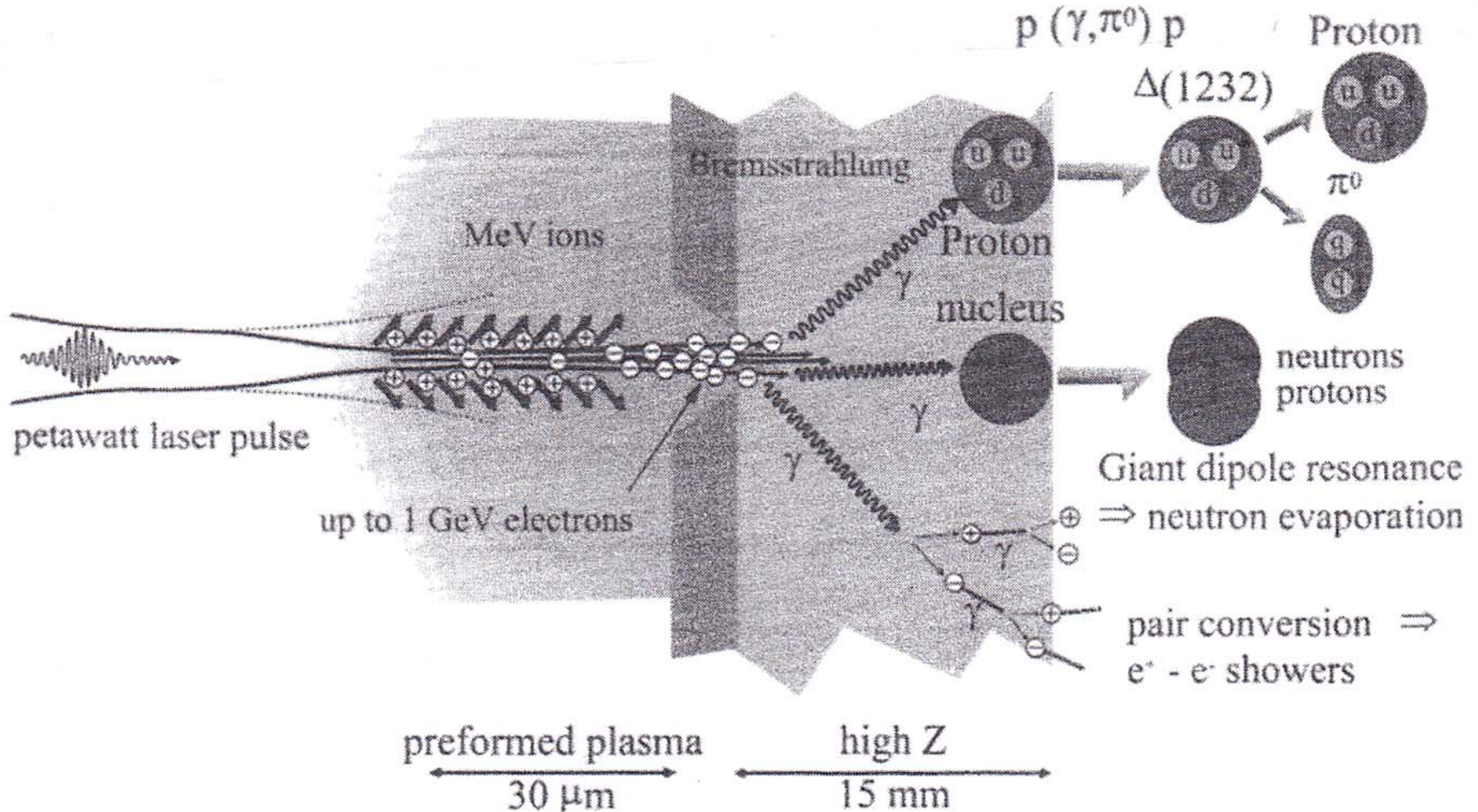


FIGURE 1. Particle production processes triggered by the large electron, ion, and  $\gamma$  fluxes which result from a petawatt laser shot focused into underdense plasma, followed by a solid target. Notice the different scales of plasma and the solid region.

# HIGH ENERGY REB ( $\gamma_b \gg 1$ )

- Less initial intensity requested
- Easier ‘piercing’ through electromagnetic instabilities
- Novel stopping mechanisms available
- Strong Langmuir stopping efficient at  $\gamma_b \gg 1$
- Huge number of possible collisional stopping channels available

## GROWTH RATES OF E.M. INSTAS DECREASE WITH $\gamma_b$

In the beam direction, the Two-Stream instability reaches a maximum for  $Z_z \sim 1$  with maximum growth rate in  $\omega_p$  units

$$\delta^{TS} \sim \frac{\sqrt{3}}{2^{4/3}} \frac{\alpha^{1/3}}{\gamma_b}$$

In the direction normal to the beam, the Filamentation instability growth rate behaves for small  $Z_x$  as

$$\delta^F \sim \sqrt{\frac{\alpha}{\gamma_b}} Z_x, \quad Z_x = \frac{k_x V_p}{\omega_p}$$

and then saturates for  $Z_x \gg \beta$  at

$$\delta^F \sim \sqrt{\frac{\alpha}{\gamma_b}}$$

Absolute maximum growth rate for oblique wave vector with  $Z_z \sim 1$  and  $Z_x \gg 1$ . Maximum Two-Stream/Filamentation growth rate

$$\delta^{TSF} \sim \sqrt{\frac{3}{2^{4/3}} \left( \frac{\alpha}{\gamma_b} \right)^{1/3}}$$

# Strong Langmuir Turbulence

$$\theta = \text{angle} (\overrightarrow{\text{REB}}, \vec{k})$$

$W_r$  = energy density in L waves resonating/REB

A crude threshold estimate for spectra with the typical

$$k \sim \omega_e/c \text{ is } W_{\text{th}} \sim n_e T_e^2 / m_e c^2 .$$

Local REB relaxation length in turbulence is

$$L_r \sim (c/2\omega_e)(m_e c^2 / T_e)^2 (\gamma_b \Delta\theta)^2 (W_{\text{th}} / W_r).$$

For  $\omega_e \sim 6 \times 10^{17} \text{ sec}^{-1}$  and  $T_e \sim 5 \text{ keV}$ , this simplifies to

$$L_r \sim 2.5(\gamma_b \Delta\theta)^2 (W_{\text{th}} / W_r) \mu\text{m}.$$

If  $W_r > W_{\text{th}}$ , this length would not exceed  $50 \mu\text{m}$  for

$$\gamma_b \Delta\theta \leq 5.$$

V M Malkin and N J Fisch PRL89,125004(2002)

T Yabuuchi et al New J Phys 11,093031(2009)

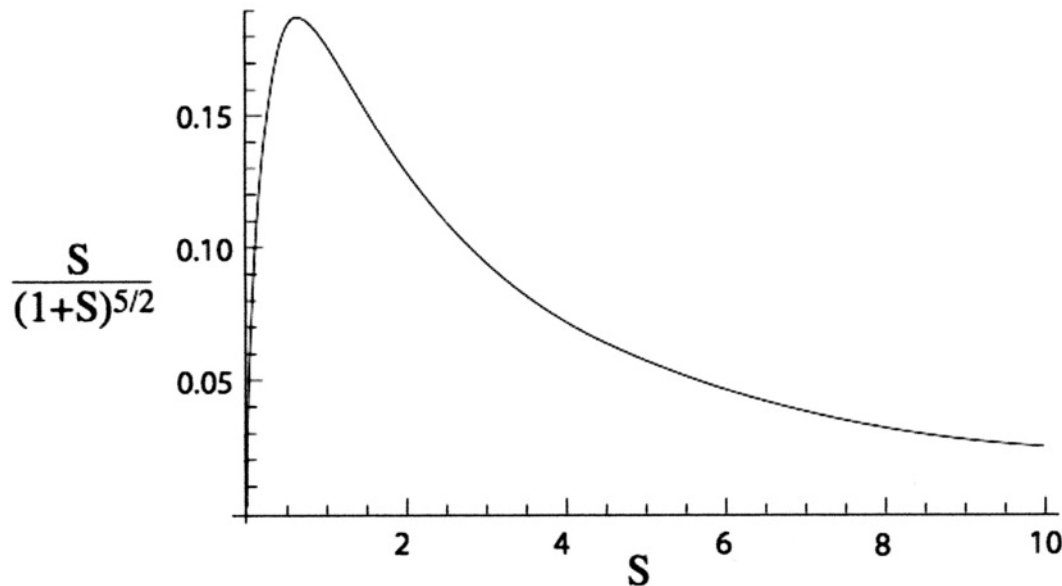
## REB STOPPING THROUGH 2-STREAM INSTABILITY

Based upon a single wave approximation in which the wave is assumed to reach its maximum amplitude instantaneously, a semi quantitative analytic solution for the fraction of beam energy converted into electric field energy is predicted to be

$$W \equiv |E|^2 / 16\pi n_b \gamma_b m c^2 = 0.5 S(1+S)^{-5/2} \sim 10\% \text{ of initial beam energy at } E_b \sim \text{MeV}$$

where  $\beta_b \gamma_b (n_b / 2n_p)^{1/3}$  is the strength parameter and  $\gamma_b = v_b / c$

cf L.E. Thode. Phys. Fluids **19**, 305 (1975)



Maximum at  $E_b = 15 \text{ MeV}$  for  $\frac{n_b}{n_p} \sim 10^{-4}$

Maximum at  $E_b = 200 \text{ MeV}$  for  $\frac{n_b}{n_p} \leq 10^{-7}$

# REB STOPPING THROUGH SHOCK IN INHOMOGENEOUS PLASMA

cf S.K. Yadav *et al.* POP **16**, 040701 (2009)

- **2D EMHD**

- **Net Energy Dissipation Rate over Length L**

$$Q \sim K L b^2 a^2 V_b$$

$$= \frac{B^2}{4\pi} \pi a^2 V_b = I^2 \frac{V_b}{c^2} = R I^2$$

with

k = inverse of normalized density scale length

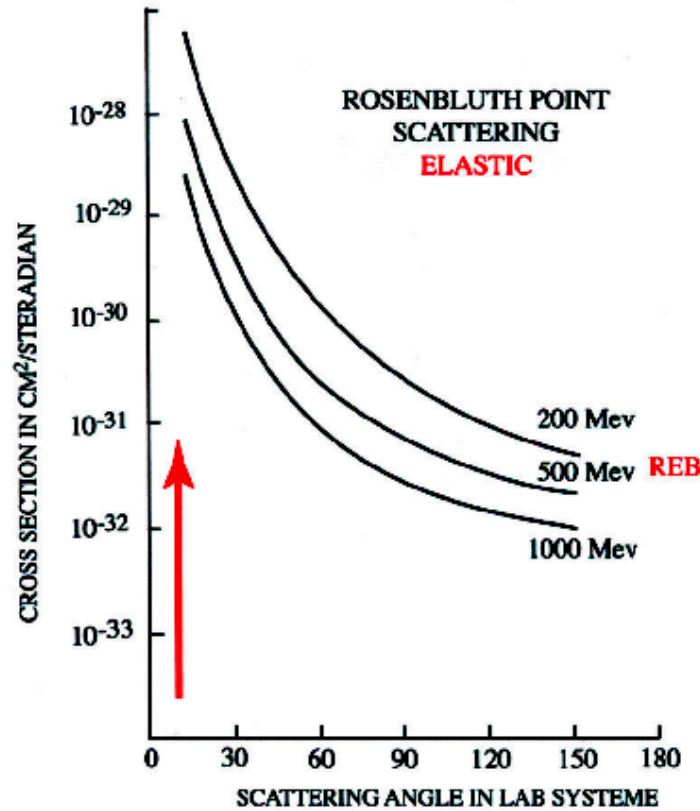
b = normalized B in x -z plane

a = channel dimension

**I = 300 kA at  $E_b = 10$  MeV can thus get stopped**



# REB Stopping on Target Ions



Rosenbluth-point scattering for point-protons with real values of nuclear spin and magnetic moment. The appropriate cross section is given with  $K = 1.79$  nuclear magnetons,  $\mu_p = 2.79$  n.m. by

$$\left(\frac{d\sigma}{d\Omega}\right)_R = \left(\frac{e^2}{2E_0}\right)^2 \frac{\cos^2 \theta/2}{\sin^4 \theta/2} \frac{1}{1 + \frac{2E_0}{Mc^2} \sin^2 \theta/2}$$

$$\left\{ 1 + \frac{\hbar^2 q^2}{4M^2 c^2} \left[ 2(1+K)^2 \tan^2 \theta/2 + K^2 \right] \right\}$$

$$(\mu_p = 1 + K = 2.79 \text{ n.m.})$$

# REB STOPPING ON TARGET ELECTRONS

The following expression has been obtained as a careful pseudoanalytic fit to quantum stopping results. It is essentially accurate for  $n_e \lesssim 10^{26} \text{ e-cm}^{-3}$ , as evidenced from stopping data.

$$-\frac{dE_b}{dx} = \frac{4\pi n e^4}{m v^2} \ln\left(\frac{2mc^2 \gamma_b^2}{\hbar \omega_p}\right)$$

K Starikov and C. Deutsch, PRE 71, 026407 (2005)

Equivalent section efficace (cross section)

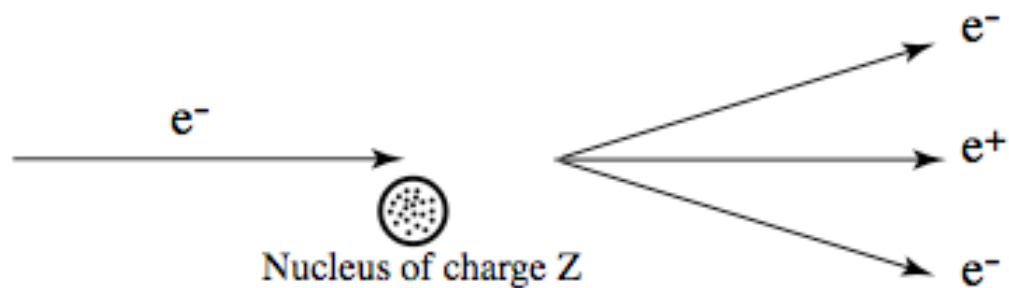
$$-\frac{dE_b}{dx} \left(\frac{\text{MeV}}{\text{cm}}\right) = n * E_b * 2.5 \times 10^{-25} \text{ cm}^2$$

equivalent  $\sigma$

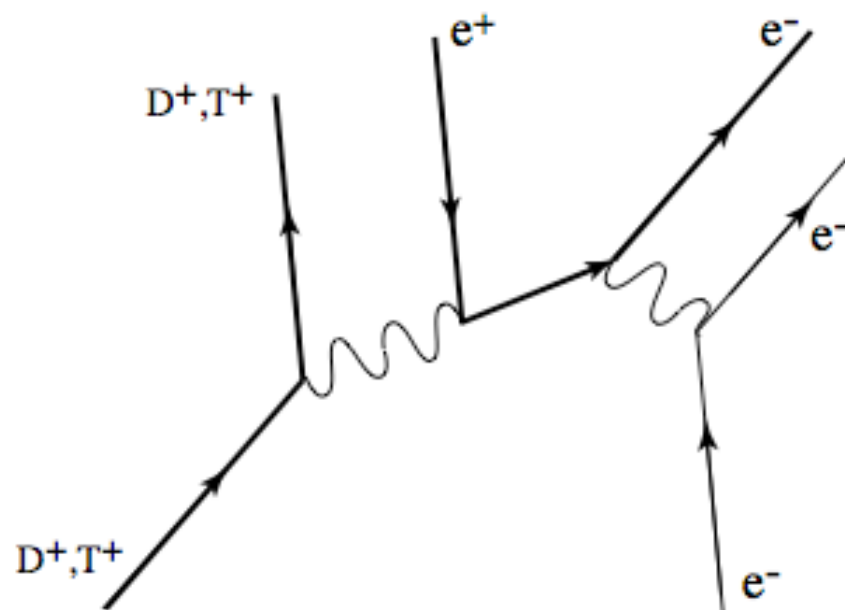
100 times Trident process for  $E_b = 200 \text{ MeV}$ .

→  $R(\mu\text{m}) = 259 \text{ at } 15 \text{ MeV}$

24 at 1 MeV

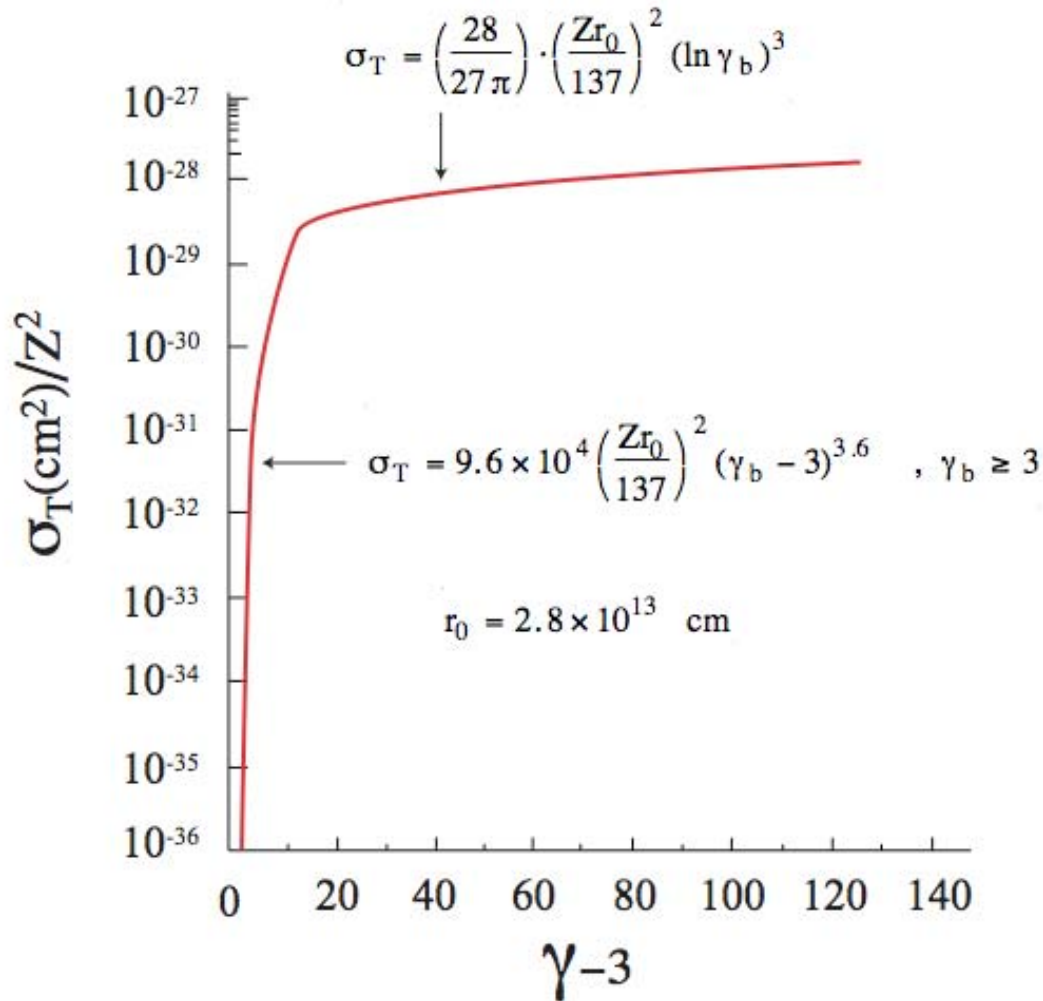


Schematic of trident process of pair creation



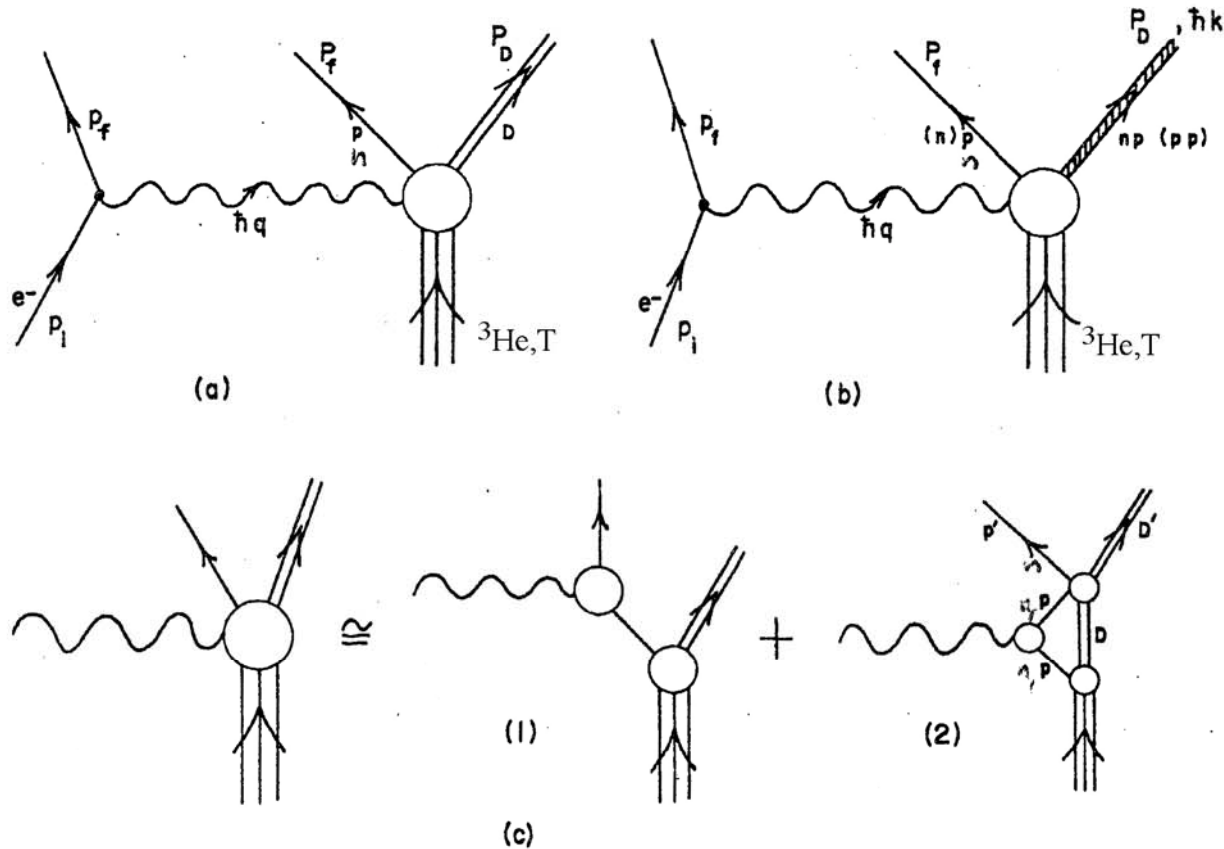
A Feynman graph contributing to [Trident production](#)

$$e + \overset{D}{T} \longrightarrow e + e + \bar{e} + \overset{D}{T}$$



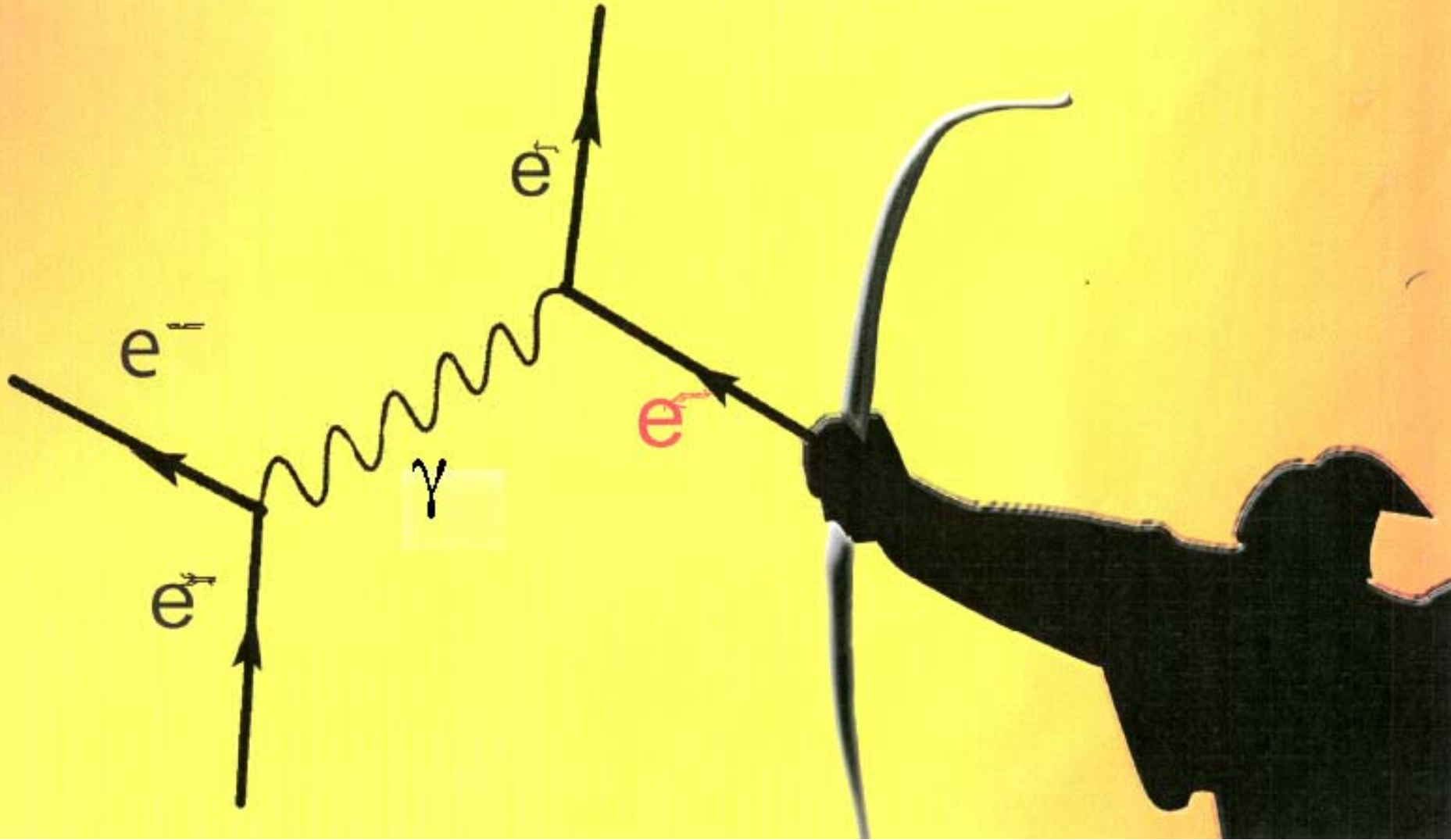
**Total cross section**  $\sigma_T$  of the trident process plotted vs the dimensionless electron-energy excess above the threshold. Here  $\gamma = E/m_0c^2$ .

# Quasielastic Electron Scattering from ${}^3\text{He}$ and ${}^3\text{H}$

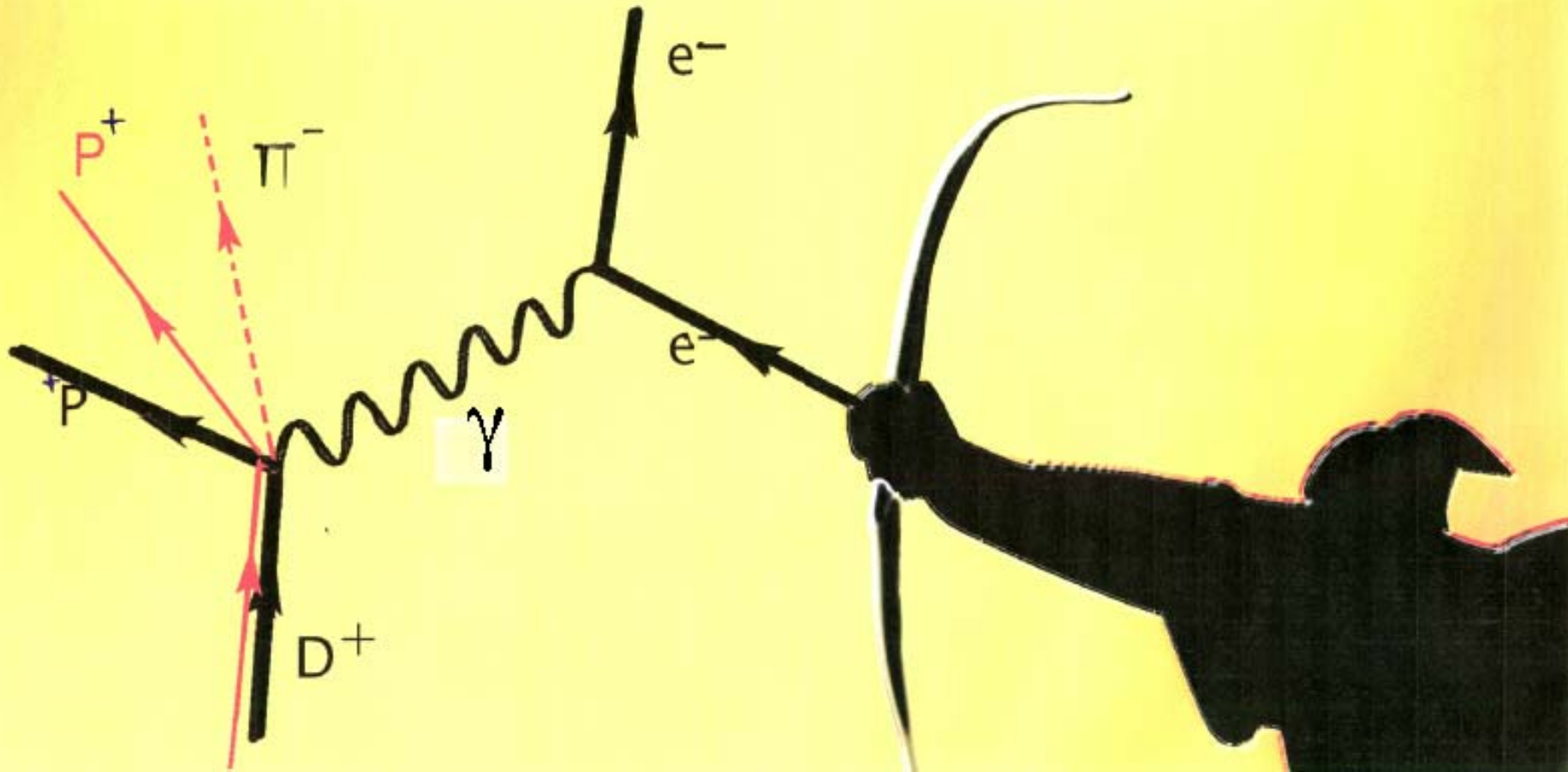


Typical graphs in electrodisintegration of  ${}^3\text{He, T}$ , (a) and (b) show the one-photon-exchange two- and three-body breakup of  ${}^3\text{He, T}$ , (c) shows the decomposition of the  $p$ - $D$ - ${}^3\text{He}$  nuclear vertex into the proton pole (1) and a correction to the proton pole (2). All intermediate states are on the mass shell.

# Möller Diagram

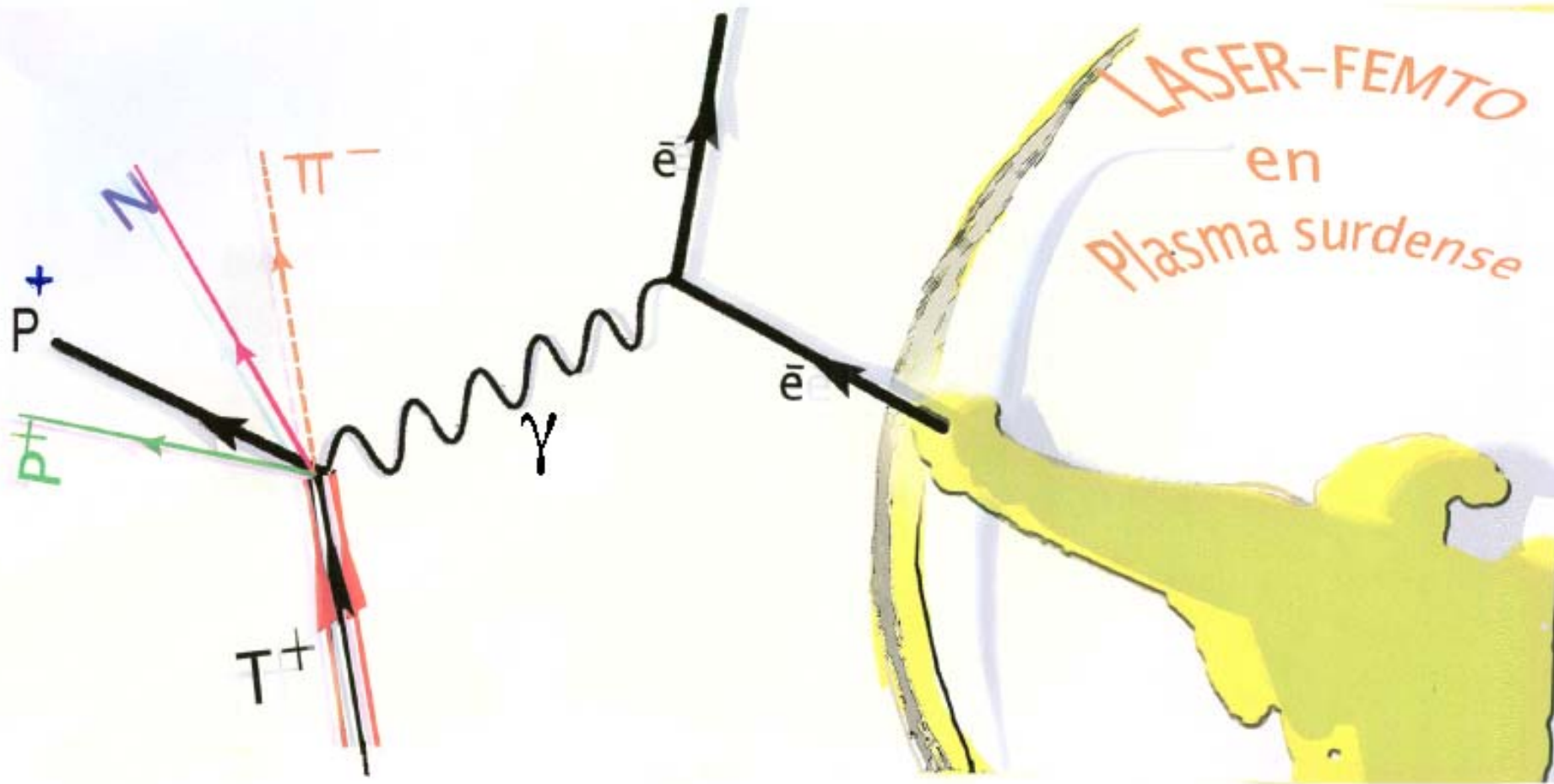


# $D^+$ Electro disintegration



One virtual Gamma only up to 1 GeV

# $T^+$ Electro-Disintegration





# nS-state pion capture fractions in hydrogen

M. Leon and H.A. Bethe, *Phys. Rev.* **127**, 636 (1962)

Capture on level  $n \sim (M_\pi/M_e)^{1/2} \sim 16$  and cascade down  $\rightarrow n = 1$

Principal quantum number n S-state capture fraction

n	
7	0.003
6	0.013
5	0.09
4	0.44
3	0.39
2	0.04

# REB-Hard Gamma Conversion

- Cone target allows for electro as well as DT fuel disintegration

Hard Gammas easily secured through REB bremsstrahlung in gold with

$$\frac{dE/dx)_{\text{rad}}}{dE/dx)_{\text{coll}}} = E_{\text{REB}} Z/1600 mc^2$$

$$=1 \rightarrow E_{\text{REB}} = 10.35 \text{ MeV in Au}$$

$$\searrow E_{\text{REB}} = 817.16 \text{ in } Z=1 \text{ DT}$$

# CONTRIBUTION TO D- and T – PHOTO DISINTEGRATION THROUGH

## REB-BREMSSTRAHLUNG IN Au (Z = 79)

$$Z^2 n_i = \frac{Z^2 \rho N_A}{A} \sim 3.66 \times 10^{26} \text{ e}^- \text{ cm}^{-3} \quad \# \quad Z^2 n_e \sim 10^{26} \text{ e}^- \text{ cm}^{-3}$$

$$\frac{\sigma_T}{\sigma_{\gamma \rightarrow e^+ e^-}} = \frac{\alpha}{\pi} \left[ \log \left( \frac{E_0}{m_e c^2} \right) \log \left( \frac{E_0}{2.137 m_e c^2 Z^{-1/3}} \right) + \frac{1}{3} \log^2 (2.137 Z^{-1/3}) \right],$$
$$= 0.017 \text{ at } 5 \text{ MeV}$$

H.J. Bhabha, Proc. R. Soc. London A **152**, 559 (1935), cf. J Myatt *et al.* POP **79**, 066409 (2009).

# $\pi^-$ Catalyzed Fusion in FIS Conditions

- $\pi^-$  production Cost  $\sim 150$  MeV  $\ll$  5.2-8 GeV in cold  $\mu$  CF
  - $\sigma_{\pi-N}$  ( $a \sim -0.036$  fm)  $\ll$   $\sigma_{N-N}$  ( $a \geq 1-8$  fm)
- ⇓
- **Catalytic cycle Mostly electromagnetic**
  - $\pi$ -D,  $\pi$ -T ground state hadronically shifted only by 0.022 percent!!
  - Cycling rate ( $n_e \sim 10^{26}$  e-cm $^{-3}$ )  $\geq 10^3$  cold cycling rate ( $n_{\text{LHD}} \sim 4.25 \times 10^{22}$  e-cm $^{-3}$ )
  - **Reduced final pion alpha sticking in hot, dense plasma.**

# Relevant lengths

$$n_e \sim 10^{26} \text{ e-cm}^{-3} \quad T \sim 1 \text{ keV}$$

$$a_{ii} = \left( \frac{4}{3} \pi n_i \right)^{-1/3} \sim 1.33 \times 10^{-9} \text{ cm}$$

Debye length  $\sim 2.35 \times 10^{-9} \text{ cm}$

Bohr radius (electron) =  $5.29 \times 10^{-9} \text{ cm}$ .

Bohr radius (pion) =  $1.94 \times 10^{-11} \text{ cm}$

$\pi$ -D and  $\pi$ -T atoms hardly affected  
by electron Debye-screening.

Considering an ignition plasma ( $N \sim 10^{26}/\text{cc}$ ,  $T \sim 3-5 \text{ KeV}$ ) in a Debye approximation demonstrates a persistence of pionic molecular ions  $\pi^- \text{D}^+ \text{T}^+$  with 319.13 eV binding energy for vibrational number  $V = 0$  and total angular momentum number  $J = 0$ , wrt to  $\text{D}^+ - \pi^-$  and  $\text{T}^+ - \pi^-$ . Such bound systems are equivalent to excited atoms with main quantum number  $N = 12$  and exhibiting anisotropy due to a nearby  $\text{D}^+$  or  $\text{T}^+$  ion.

$N = 12$  remains out of immediate nuclear capture

# BORROMEAN STABLE CONFIGURATIONS

$$DT_{\Pi}, DD_{\Pi}, TT_{\Pi}, DT_{\Pi\Pi}, DD_{\Pi\Pi}, T_{\Pi\Pi},$$

Let us number the particles in such a way that the following inequalities are valid for their masses:

$$m_1 \geq m_2, \quad m_3 \geq m_4, \quad m_2 \geq m_4.$$

With this numbering of particles the lowest dissociation threshold for the four-particle system,  $E_{th}$ , in the system of Hartree atomic units ( $\hbar=1$ ,  $m_e=1$ ,  $q_e=1$ ) is

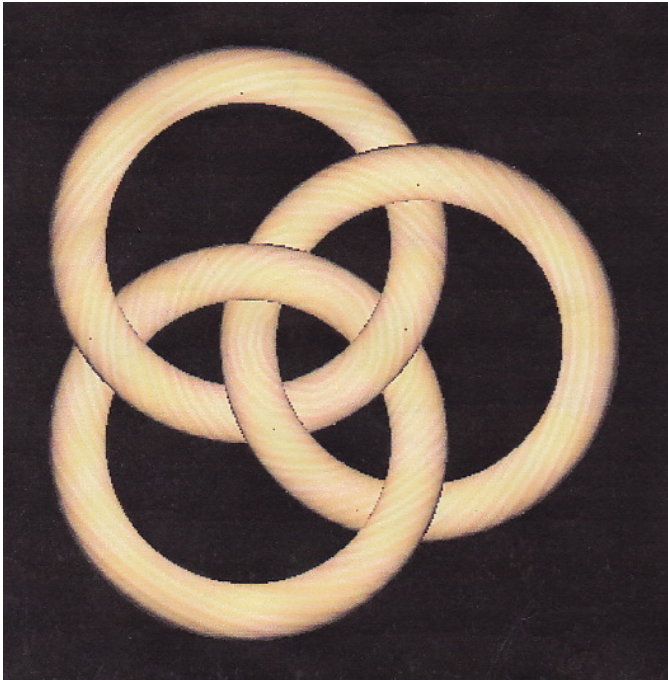
$$E_{th}(m_1^+ m_2^+ m_3^- m_4^-) = -\frac{m_1 m_3}{2(m_1 + m_3)} - \frac{m_2 m_4}{2(m_2 + m_4)}$$

while the lowest dissociation (ionization) threshold for the three-particle system is

$$E_{th}(m_1^+ m_2^+ m_3^-) = -\frac{m_1 m_3}{2(m_1 + m_3)}$$

$$s = \left( \frac{1}{m_1} + \frac{1}{m_3} \right) / \left( \frac{1}{m_2} + \frac{1}{m_4} \right)$$

$$0.4710 \leq s \leq 2.1231 \quad \text{Stable}$$



## BORROMEAN CONFIGURATIONS

$T^+ D^+ \pi^- e^-$  system ( $s = 0.0007$ ) unstable

In these Borromean schemes,  $DT_{\pi}, DT_{\pi\pi} \dots$  with  $s \cong 1$  are stable.

This system can bind one more electron forming  $(M^+, M^+, x^-, e^-, e^-)$ , which is akin to  $H^-$ . A possible choice of  $x^-$  is  $\pi^-$ . The  $(p, p, \pi^-)$  system is bound, and the  $(p, p, e^+, \pi^-)$  and  $(p, p, e^-, e^- \pi^-)$  systems are also bound. These systems remain bound even if the masses of the heavy particles are slightly different, e.g., the  $(M_1^+, M_2^+, e^-, e^-, x^-)$  system is bound as a rough estimate for  $1/3 < M_1/M_2 < 1$ .



$$\frac{m_D}{m_T} \sim 2/3$$

In a mostly electron-screened target, mesomolecules appear nearly Coulombian



## DEBYE-SCREENED MOLECULES

$$V(r_a, r_b) = q_a q_b \exp\left(\frac{-|r_a - r_b|}{D}\right) / |r_a - r_b| .$$

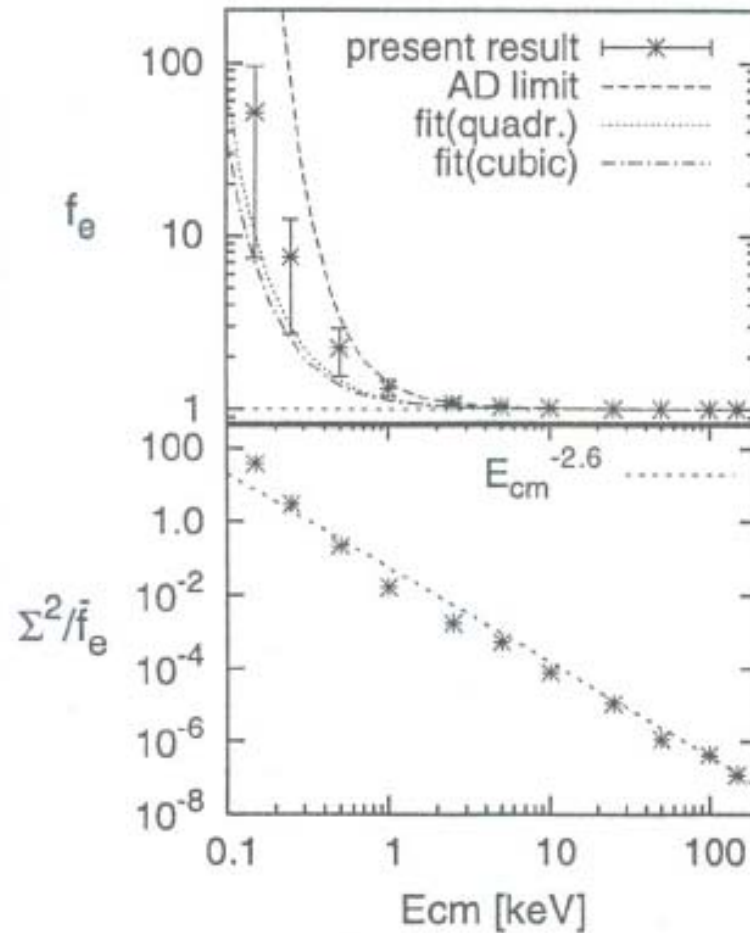
$$H = -\frac{1}{2m_1} \nabla_1^2 - \frac{1}{2m_2} \nabla_2^2 - \frac{1}{2m_3} \nabla_3^2 + V(r_3, r_1) + V(r_3, r_2) + V(r_2, r_1) ,$$

Ground and excited states energies of plasma-embedded  $td_\mu$  molecular ion for different screening parameter along with the  $n = 1$  threshold energies of  $t\mu$ . Quoted results are in m.a.u.

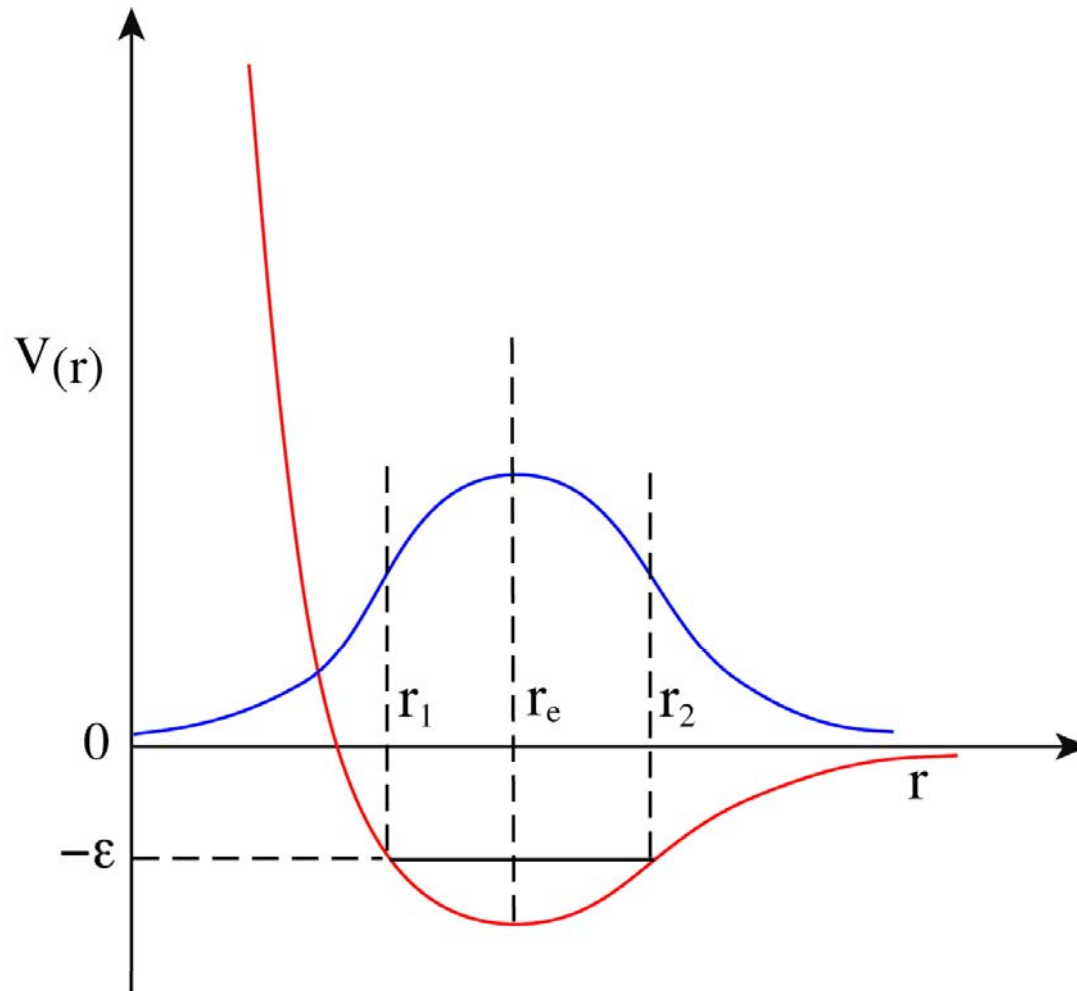
D	$t\mu$ ( $n=1$ )	$td_\mu$ ( $J=0, v=0$ )	$td_\mu$ ( $J=0, v=1$ )
$\infty$	-0.481874166748	-0.538594975	-0.488065358
100	-0.471951457103	-0.528664171	-0.478140323
50	-0.462181262989	-0.518869867	-0.468363045
30	-0.449386465096	-0.506018492	-0.455551309
20	-0.433756779919	-0.490279822	-0.439888656
15	-0.418520153061	-0.474893060	-0.424606668
10	-0.389182419992	-0.445137640	-0.395145273
8	-0.368133808415	-0.423678964	-0.373979717
6	-0.334783387306	-0.389475264	-0.340399609
5	-0.309590742305	-0.363459345	-0.315000779
4	-0.274153085855	-0.326575303	-0.279231352
3	-0.220971475522	-0.270488395	-0.225474576
2.5	-0.183360941776	-0.230169921	-0.187411245
2.0	-0.134547882290	-0.176754630	-0.137964289
1.5	-0.071690979839	-0.105039966	-0.074215725
1.2	-0.029655544877	-0.052965468	-0.03145845
1.1	-0.0168475687	-0.035286667	-0.0183319
1.0	-0.00634745	-0.018756598	-0.00739
0.9	-0.000378	-0.0053050	-0.00046
0.89	-0.00016	-0.0042584	

Larger systems are better armed to survive screening

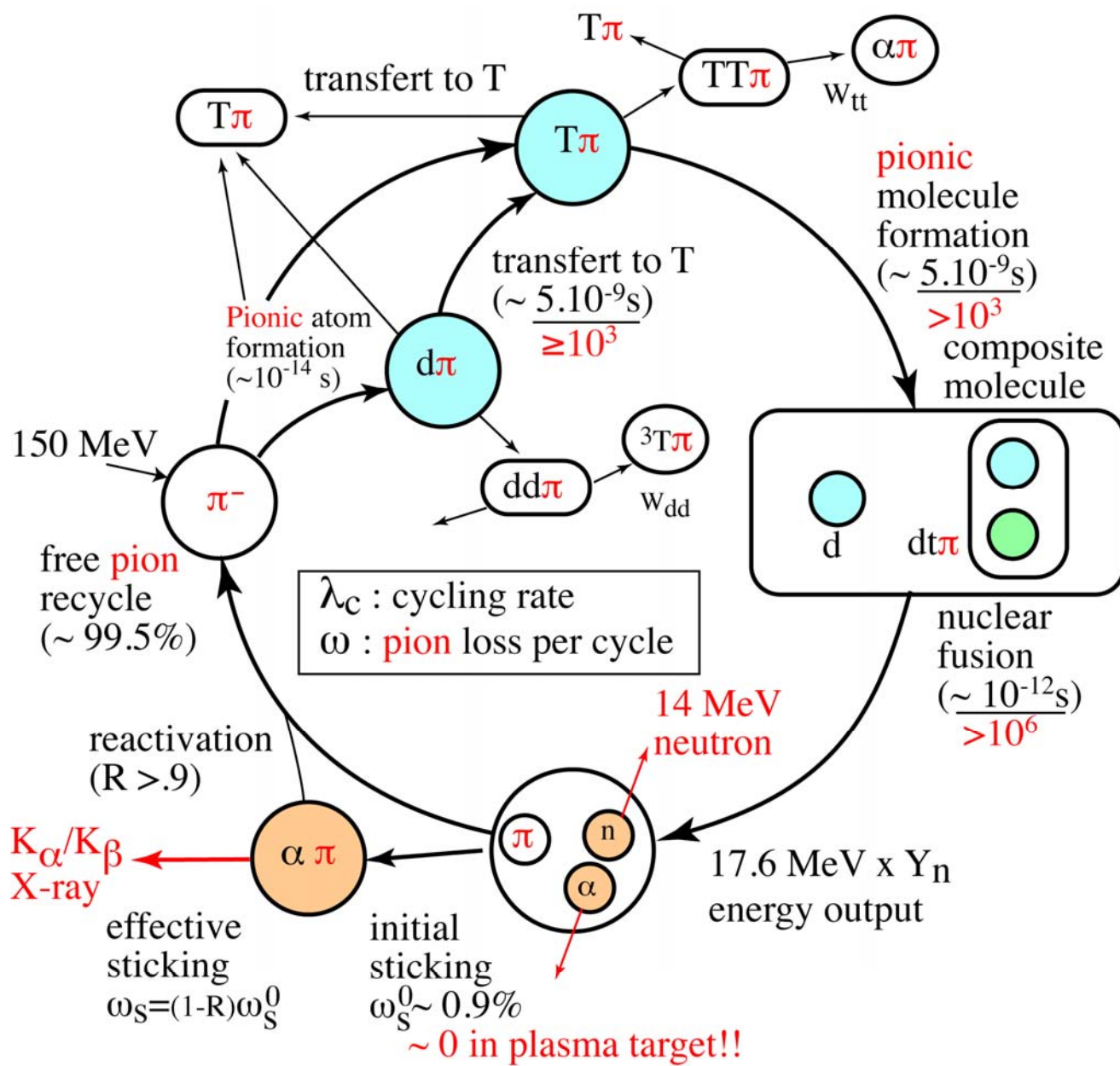
# Chaotic Nuclei Screening Coulomb Barrier Lowered by 2 Orders of Magnitude



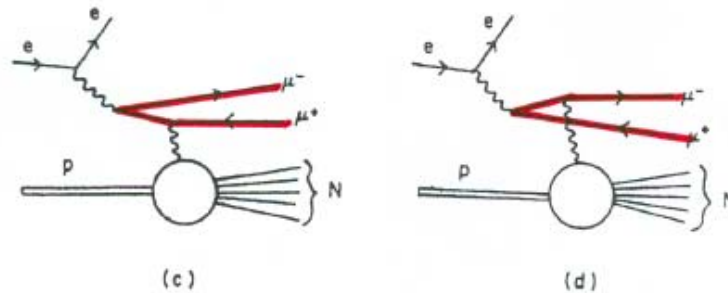
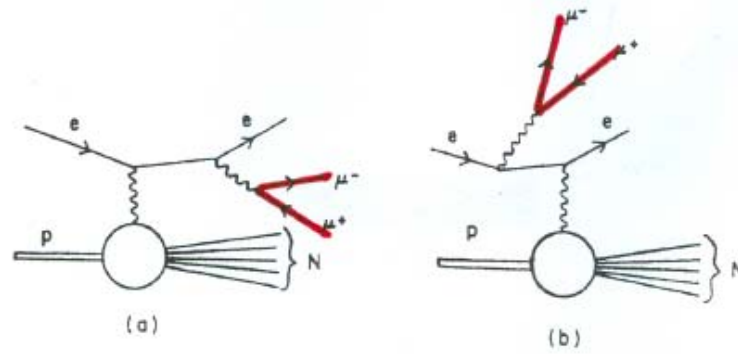
Enhancement factor as a function of incident center-of-mass energy for the  $D + d$  reaction (upper panel). The corresponding  $\Sigma^2/\bar{f}_e$  (stars) and a power-law fit (dashed line) (lower panel).



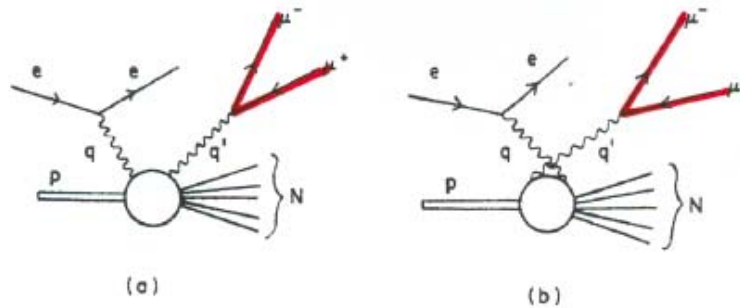
Nuclear potential energy curve in  $\pi$ -mesonic hydrogenic molecule, and ground-state vibrational wave function for the while  $r_1$  and  $r_2$  are the classical turning points. The bound state energy level is  $-\epsilon$ .



Possible diagram of the **pion** catalyzed fusion cycle in FIS conditions



Lowest-order Bethe-Heitler-type diagrams contributing to the process  $e+p \rightarrow e+\mu^-+\mu^+$  + "anything." The contribution of such diagrams to the cross section can be calculated in terms of structure functions  $W_1$  and  $W_2$ .



Lowest-order Compton-type diagrams contributing to the process  $e+p \rightarrow e+\mu^-+\mu^+$  + "anything."

# PROVISIONAL SUMMARIES

- Strong Langmuir turbulence and inelastic high energy REB offer new prospects for FIS/ICF.
- Pion catalyzed fusion could provide substantial contributions: cheaper, faster and No sticking.
- Discontinuous REB stopping through  $\gamma$ -and  $(e^+e^-)$  pair productions remain to be explored.
- $\pi^-$  stopping needs more investigation.

Production of Borromean molecular states via  $(e^-e^+)$  decay into Wheeler complexes  $ne-me^+$  and  $\text{Pi}^-$  catalysis out of DT electro and photodisintegration (cone target)